HEAVY-FLAVOR PRODUCTION IN THE CMS*

Byungsik Hong

on behalf of the CMS Collaboration

Department of Physics, Korea University, Seoul 136-701, Korea

(Received December 12, 2011)

The compact muon solenoid (CMS) detector at the large hadron collider (LHC) is ideal to measure the heavy flavor production, especially, in the dimuon channels in high-multiplicity environment. Compared to the *pp* data scaled by the number of binary collisions, the yields of prompt and non-prompt J/ψ and $\Upsilon(1S)$ in Pb–Pb collisions are strongly suppressed at $\sqrt{s_{NN}} = 2.76$ TeV. In addition, the excited $\Upsilon(2S{+}3S)$ states are also suppressed relative to the ground $\Upsilon(1S)$ state in Pb–Pb collisions. These results consistently indicate a significant medium effect on the heavy-flavor production in heavy-ion collisions at LHC.

DOI:10.5506/APhysPolB.43.517
PACS numbers: 25.75.–q, 14.40.Pq, 14.65.Dw, 14.65.Fy

1. Introduction

The theory of strong interaction, quantum chromodynamics (QCD), predicts the deconfined partonic matter or the quark-gluon plasma (QGP) in heavy-ion collisions at high energies. While they propagate in the medium, various quarkonium states produced at early stage are expected to be dissolved sequentially, depending on their binding energies, due to Debye screening [1]. As a result, the quarkonium production in heavy-ion collisions, in principle, provides valuable information on not only the formation of QGP, but also the detailed properties of QCD in dense matter.

However, there are several complications at various levels to interprete the heavy-ion data. First of all, there are presently no satisfactory model which can describe simultaneously the production cross section and the polarization of quarkonium in *pp* collisions. Secondly, the cold nuclear matter effects, such as shadowing and gluon saturation, in the initial state

* Presented at the Conference "Strangeness in Quark Matter 2011", Kraków, Poland, September 18–24, 2011.

play an important role, but there are no detailed information available with enough precision yet [2]. Finally, a similar J/ψ suppression at RHIC ($\sqrt{s_{NN}} = 200$ GeV) and SPS (17 GeV) as well as a larger suppression at forward rapidity than at midrapidity in Au–Au at RHIC remain as puzzles [3]. As a result, the quarkonium production data in pp as well as heavy-ion collisions at much higher LHC energies are expected to aid in solving these puzzles.

In this paper, we present the prompt and non-prompt J/ψ productions in pp collisions at $\sqrt{s} = 7$ TeV. Subsequently, we present the J/ψ and Υ productions in Pb–Pb relative to them in pp at $\sqrt{s_{NN}} = 2.76$ TeV in order to elucidate the medium effects.

2. Overview of the CMS detector and data samples

The CMS detector at LHC is ideal to study the quarkonium production, especially, with the dimuon channels [4]. The CMS muon detection system consists of the drift tubes, the cathode strip chambers, and the resistive plate chambers. It covers a large acceptance for $|\eta| < 2.4$ with full azimuthal coverage outside a superconducting solenoid magnet with a field of 3.8 T. The inner tracking system, which consists of about 76 million silicon pixels and microstrips, provides a precise momentum information of muons for $|\eta| < 2.4$. The momentum resolution of muon is better than 1.5% for the transverse momentum $p_{\mathrm{T}} < 100$ GeV/c. For the centrality measurement of the heavy-ion events, the forward hadronic calorimeters in $3 < |\eta| < 5$ have been used.

The current analysis for Pb–Pb collisions at $\sqrt{s_{NN}} = 2.76$ TeV is based on a total integrated luminosity ($\mathcal{L}_{\mathrm{int}}$) of 7.28 μb^{-1}, having been taken during the first heavy-ion run in 2010. The reference pp data, corresponding to the integrated luminosity ($\mathcal{L}_{pp}$) of 225 nb^{-1}, were collected at the same beam energy in March 2011. (Note that the integrated luminosity of the pp data is roughly the same as the number of binary collision scaled Pb–Pb data.) In addition, the J/ψ spectra in pp collisions at $\sqrt{s} = 7$ TeV to be presented in the next section are based on $\mathcal{L}_{pp} = 36.7$ pb^{-1}.

3. Heavy-flavor production in *pp* at $\sqrt{s} = 7$ TeV

The measured J/ψs are classified into the prompt component associated with the primary vertex and the non-prompt component associated with the secondary vertex. The non-prompt J/ψs are generated from decays of the B mesons whereas the prompt J/ψs are originated from either the direct production or the feed-down of higher states such as ψ' and χ_c. As the B mesons fly finite pathlength before decay, the non-prompt J/ψs can be separated from the prompt ones by using the pseudo-proper decay length, $l_{J/\psi} = L_{xy}\, m_{J/\psi}/p_{\rm T}$, where L_{xy} is the distance between the primary and the secondary vertices in the transverse plane. CMS has fitted the invariant mass and the pseudo-proper decay length distributions simultaneously. An example of the invariant mass and the projected $l_{J/\psi}$ distributions of $\mu^+\mu^-$ pairs in forward rapidity ($1.6 < |y| < 2.4$) in pp collisions at $\sqrt{s} = 7$ TeV is shown in Fig. 1 [5].

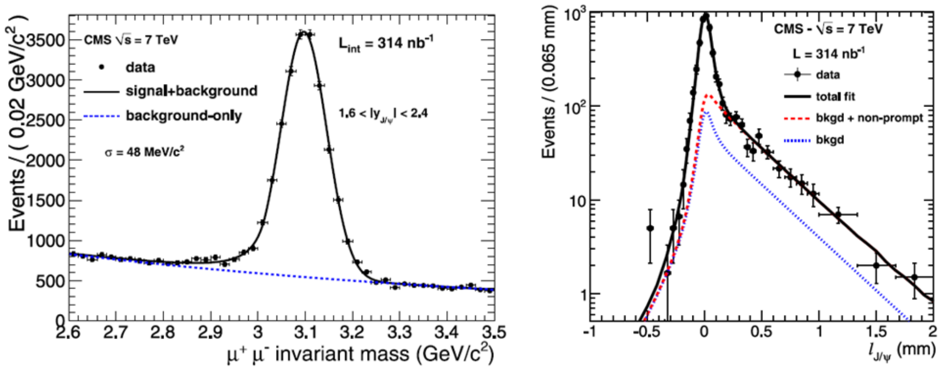

Fig. 1. Invariant mass (left) and pseudo-proper decay length (right) distributions of $\mu^+\mu^-$ pairs in forward rapidity ($1.6 < |y| < 2.4$) in pp collisions at $\sqrt{s} = 7$ TeV [5]. In the left panel, the solid line represents the sum of the 'crystal ball' function for signal and an exponential function for background. In the right panel, the dotted and dashed lines represent the background and the non-prompt J/ψ component, respectively, and the solid line is the total fit function including the prompt J/ψ component.

Figure 2 shows the measured cross sections of the prompt and non-prompt J/ψ as a function of $p_{\rm T}$ for the several rapidity bins in pp collisions at $\sqrt{s} = 7$ TeV [6]. The data are compared with the theoretical calculations (NRQCD for the prompt and FONLL for the non-prompt components), and good agreement can be found except that the non-prompt spectra fall more rapidly than the model calculations at high $p_{\rm T}$. For $\psi(2S)$s, the comparison between the model calculations and the data show a similar level of agreement as J/ψ except an overall scale difference for the non-prompt component possibly due to the large uncertainty of the decay rate for $B \to \psi(2S)$ [6].

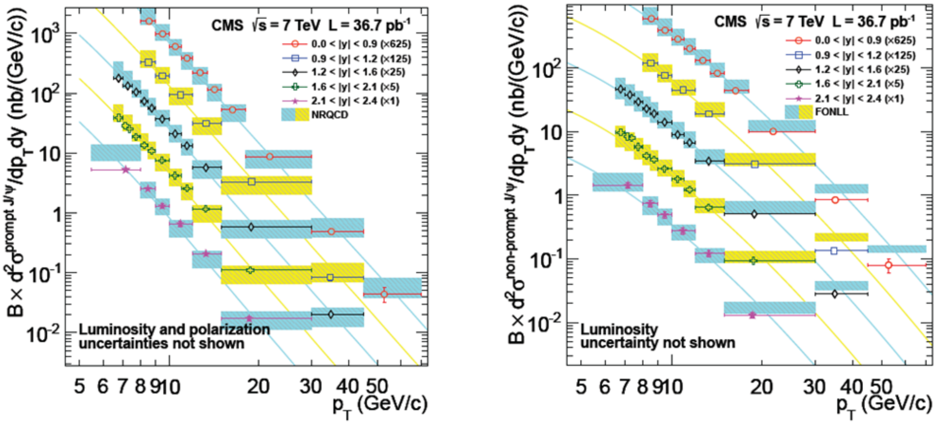

Fig. 2. Cross sections of the prompt (left) and non-prompt (right) J/ψs as a function of p_{T} for the several rapidity bins in pp collisions at $\sqrt{s} = 7$ TeV [6]. (Note that the p_{T} reaches up to 70 GeV$/c$.) The bars on data points include all statistical as well as systematic errors except the contributions from luminosity and polarization. The grey (coloured) boxes represent the theoretical predictions from the QCD models.

4. Heavy-flavor production in Pb–Pb at $\sqrt{s_{NN}} = 2.76$ TeV

At $\sqrt{s_{NN}} = 2.76$ TeV, using the J/ψ raw yields, which are to be denoted as $N_{\mathrm{Pb-Pb}}(J/\psi)$ and $N_{pp}(J/\psi)$ for Pb–Pb and pp collisions, respectively, the nuclear modification factor is analyzed by

$$R_{AA} = \frac{\mathcal{L}_{pp}}{T_{AA} N_{\mathrm{MB}}} \frac{N_{\mathrm{Pb-Pb}}(J/\psi)}{N_{pp}(J/\psi)} \frac{\epsilon_{pp}}{\epsilon_{\mathrm{Pb-Pb}}}\,, \tag{1}$$

where T_{AA} is the nuclear overlap function estimated by the Glauber model, N_{MB} is the counted number of equivalent minimum bias events in Pb–Pb, and $\epsilon_{pp}/\epsilon_{\mathrm{Pb-Pb}}$ is the multiplicity dependent ratio of the efficiencies in pp and Pb–Pb collisions for trigger and reconstruction. The ratio, $\epsilon_{pp}/\epsilon_{\mathrm{Pb-Pb}}$, has been determined by Monte Carlo simulations which embedded a PYTHIA signal event to a HYDJET background event, and estimated as about 1.17 for the most central bins. Deviation of Eq. (1) from unity indicates the medium effect on the J/ψ production in Pb–Pb collisions.

The nuclear modification factors of prompt J/ψs as functions of p_{T}, N_{part} (the number of participating nucleons determined by the Glauber model), and y are displayed in Fig. 3 [7]. A factor of 3 suppression is observed for two p_{T} bins when integrated over all centralities and rapidities. However, a large centrality dependence can be observed for $6.5 < p_{\mathrm{T}} < 30.0$ GeV$/c$ as the suppression factor decreases from ~ 5 for the most central 10% to ~ 1.6

for 50–100% centrality bin. These observations are contrasted to the RHIC data measured at $\sqrt{s_{NN}} = 200$ GeV as shown in the left panel of Fig. 3. The RHIC data for $p_{\mathrm{T}} \lesssim 4$ GeV/c show a similar level of suppression as the CMS data, but it approaches unity at higher p_{T}, which results in a strong beam-energy dependence at $p_{\mathrm{T}} > 6.5$ GeV/c. Furthermore, CMS shows that the yield of prompt J/ψs is less suppressed at forward rapidity than at midrapidity for $p_{\mathrm{T}} > 6.5$ GeV/c which is opposite to what PHENIX has observed at lower p_{T}. The difference between the CMS and the RHIC data may come from the (anti-)shadowing effect for different x ranges covered and/or the different amount of the regeneration contribution. However, the quantitative interpretation is yet to come.

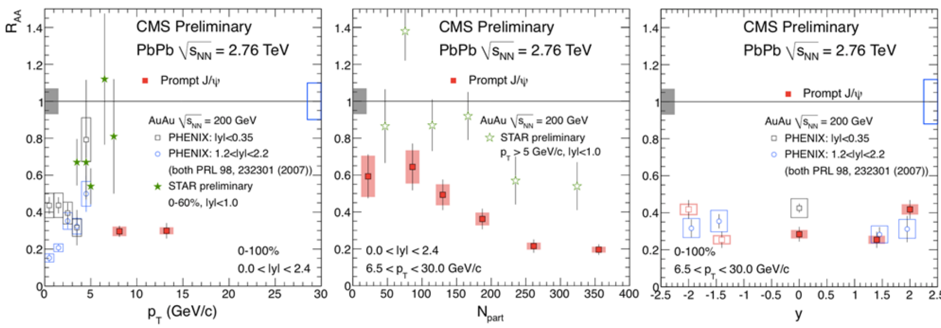

Fig. 3. Transverse momentum (left), centrality (middle), and rapidity (right) dependences of the nuclear modification factor of prompt J/ψs at $\sqrt{s_{NN}} = 2.76$ TeV [7]. The grey box at $R_{AA} = 1$ represents a global scale uncertainty (8.3%) originated from the determination of T_{AA} and the measured integrated luminosity of the *pp* data sample. The CMS data are compared to the PHENIX ($|y| < 0.35$ by open squares and $1.2 < |y| < 2.2$ by open circles) and the STAR ($|y| < 1.0$ by stars) data measured at $\sqrt{s_{NN}} = 200$ GeV. In the right panel, the CMS data for $y < 0$ are reflections of those for $y > 0$ because of the symmetry of the collision system.

Figure 4 displays the nuclear modification factor of non-prompt J/ψ as a function of N_{part} at $\sqrt{s_{NN}} = 2.76$ TeV [7]. Non-prompt J/ψs produced in Pb–Pb collisions are suppressed by a factor of ~ 2.7 relative to the *pp* data, which is the first indication of the *b*-quark energy loss in medium. No centrality dependence is noticed with the present wide bin size (especially, the peripheral bin of 20–100%), and the data with finer centrality bins are expected using the higher statistics data sample in the future.

The excellent resolution of the CMS detector allows us to separate $\Upsilon(1S)$ from the higher $\Upsilon(2S+3S)$ states in *pp* as well as Pb–Pb collisions. Figure 5 shows the invariant mass distributions of $\mu^+\mu^-$ pairs for the p_{T} of each muon, p_{T}^{μ}, larger than 4 GeV/c in *pp* and Pb–Pb at $\sqrt{s_{NN}} = 2.76$ TeV [8].

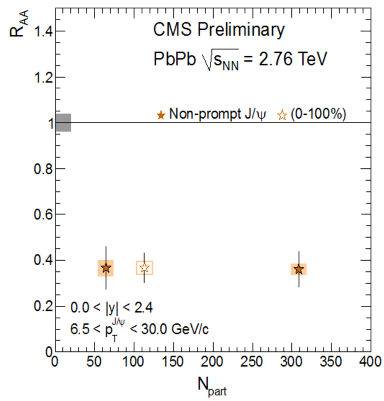

Fig. 4. Centrality dependence of the nuclear modification factor of non-prompt J/ψs at $\sqrt{s_{NN}} = 2.76$ TeV [7]. The grey box at $R_{AA} = 1$ represents a global scale uncertainty (6%) originated from the measured integrated luminosity of the pp data sample.

Likewise the J/ψ analysis, each Υ state is parameterized by a 'crystal ball' function. Since the three Υ states partially overlap in the measured mass region, a simultaneous fit with three 'crystal ball' functions added to the second-order polynomial function for the background has been performed. The solid lines in Fig. 5 represent the results of fitting.

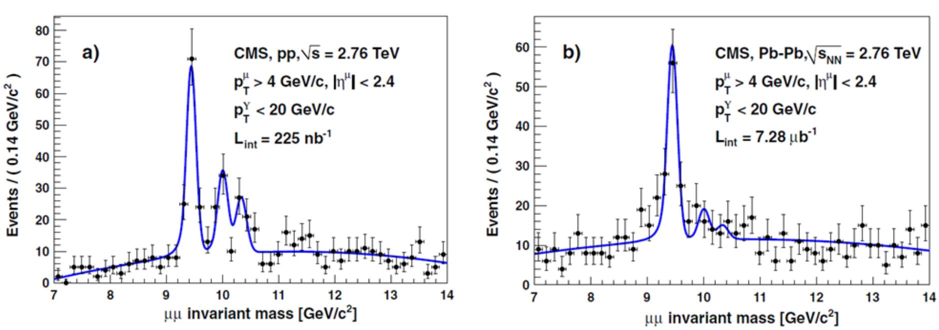

Fig. 5. Invariant mass distributions of $\mu^+\mu^-$ pairs for $p_T^\mu > 4$ GeV/c in pp (left) and Pb–Pb (right) collisions at $\sqrt{s_{NN}} = 2.76$ TeV [8]. The solid lines are the fit functions described in the text.

Comparing the dimuon invariant mass distributions in pp and Pb–Pb, the higher $\Upsilon(2S+3S)$ states are found to be suppressed with respect to the $\Upsilon(1S)$ state in Pb–Pb collisions. Fitting to the $\mu^+\mu^-$ invariant mass distributions for pp and Pb–Pb gives the double ratio

$$\frac{\Upsilon(2S+3S)/\Upsilon(1S)|_{\mathrm{Pb-Pb}}}{\Upsilon(2S+3S)/\Upsilon(1S)|_{pp}} = 0.31^{+0.19}_{-0.15}(\mathrm{stat}) \pm 0.03(\mathrm{syst})\,, \qquad (2)$$

where the systematic uncertainty arises from varying the line shape in the simultaneous fit, thus taking into account partial cancellation of systematic effects. In order to check the significance of Eq. (2), an ensemble of one million pseudoexperiments has been generated with the signal line shape obtained from the pp data in the left panel of Fig. 5, the background line shapes from both date sets, and a double ratio of Eq. (2) as unity within the statistical and systematic uncertainties. This test returns that the probability to find the measured double ratio of 0.31 or smaller is estimated to be 0.9%, which corresponds to 2.4 σ effect in a one-tail integral of a Gaussian distribution.

Figure 6 displays the nuclear modification factor of $\Upsilon(1S)$ as functions of $p_{\rm T}$, $N_{\rm part}$, and y at $\sqrt{s_{NN}} = 2.76$ TeV [7]. The $p_{\rm T}$ dependence shows the suppression by a factor of ~ 2.3 at low $p_{\rm T}$ in Pb–Pb collisions, but the suppression disappears for $p_{\rm T} > 6.5$ GeV/c. From the centrality dependence, $\Upsilon(1S)$ is suppressed by about a factor of 2 in the most central 10% bin, but the large statistical uncertainties for less central events prevent any definite conclusions on the centrality dependence yet. In Fig. 6, the $N_{\rm part}$ dependence of the CMS data are compared with the preliminary inclusive STAR data for $\Upsilon(1S{+}2S{+}3S)$ in Au+Au collisions at $\sqrt{s_{NN}} = 200$ GeV [9], showing a suppression of a similar order of magnitude despite of a large beam-energy difference. Finally, for the rapidity dependence, a slightly larger suppression at midrapidity is observed, but the large statistical uncertainties again prevent any definite conclusions yet.

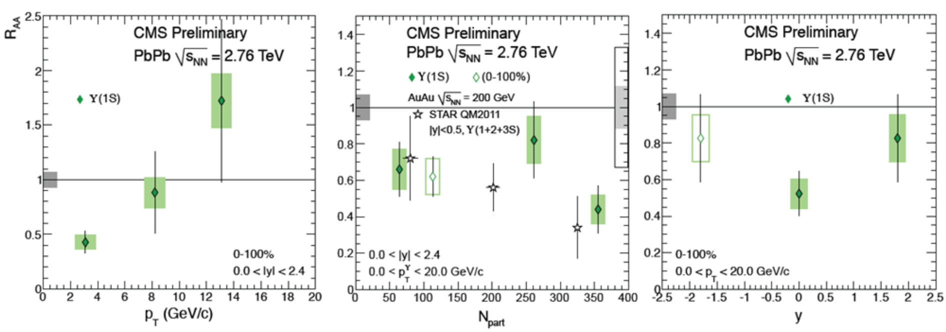

Fig. 6. Transverse momentum (left), centrality (middle), and rapidity (right) dependences of the nuclear modification factor of $\Upsilon(1S)$ at $\sqrt{s_{NN}} = 2.76$ TeV [7]. The grey box at $R_{AA} = 1$ represents a global scale uncertainty (8.3%) originated from the determination of T_{AA} and the measured integrated luminosity of the pp data sample. The CMS data in the middle panel are compared to the preliminary inclusive STAR ($|y| < 1.0$ by stars) data measured at $\sqrt{s_{NN}} = 200$ GeV [9]. In the right panel, the CMS point in the negative rapidity is the reflection of that in the positive rapidity due to the symmetry of the collision system.

5. Summary

This paper summarizes the experimental data on the productions of J/ψ and Υ via $\mu^+\mu^-$ channel in pp as well as Pb–Pb collisions, measured by the CMS Collaboration. The non-prompt J/ψs are well separated from the prompt J/ψs by fitting the invariant mass and the pseudo-proper decay length distributions simultaneously.

The prompt and non-prompt J/ψ cross sections are measured up to $p_{\mathrm{T}} = 70$ GeV/c in pp collisions at $\sqrt{s} = 7$ TeV. In general, the data are well reproduced by the QCD models except at high p_{T}, where the calculations for non-prompt J/ψ overestimate the data.

The prompt and non-prompt J/ψ cross sections are analyzed in Pb–Pb collisions at $\sqrt{s_{NN}} = 2.76$ TeV, and compared with those in pp at the same energy in order to evaluate the nuclear modification factors. The prompt J/ψ cross section is suppressed by a factor of about 5 for the 10% most central events, which diminishes to about 1.6 for the 50–100% centrality bin. No p_{T} dependence is found for prompt J/ψs with the current uncertainties, while a slight more suppression is observed at midrapidity than at forward rapidity. On the other hand, the non-prompt J/ψs decayed from the B mesons are also suppressed by a factor of about 2.7 with respect to the pp data, which indicates the energy loss by b-quarks in medium.

The $\Upsilon(1S)$ state in Pb–Pb collisions is suppressed by a factor of ~ 2 in the 10% most central events when integrated over all p_{T} and y. The suppression factor is larger at low p_{T}, and reduces to unity at larger p_{T}. The ratio of $\Upsilon(2S{+}3S)$ to $\Upsilon(1S)$ in Pb–Pb collisions is suppressed by a factor of about 3 with respect to that in pp for $p_{\mathrm{T}}^{\mu} > 4$ GeV/c. The probability to obtain the measured, or smaller, value of the double ratio, if the true suppression factor is unity, has been estimated to be about 0.9%.

This work was supported in part by the National Research Foundation of Korea under grant No. K20802011718-11B1301-00610.

REFERENCES

[1] T. Matsui, H. Sats, *Phys. Lett.* **B178**, 416 (1986).

[2] PHENIX Collaboration, *Phys. Rev.* **C77**, 024912 (2008).

[3] PHENIX Collaboration, *Phys. Rev.* **C84**, 054912 (2011) `arXiv:1103.6269v1 [nucl-ex]`.

[4] CMS Collaboration, *JINST* **0803**, 08004 (2008).

[5] CMS Collaboration, *Eur. Phys. J.* **C71**, 1575 (2011).

[6] CMS Collaboration, CMS-PAS-BPH-10-014.

[7] CMS Collaboration, CMS-PAS-HIN-10-006.

[8] CMS Collaboration, *Phys. Rev. Lett.* **107**, 052302 (2011).

[9] R. Reed [STAR Collaboration], `arXiv:1109.3891v1 [nucl-ex]`.